UCLA
UCLA Previously Published Works

Title

Similarity in functional brain connectivity at rest predicts interpersonal closeness in the social network of an entire village

Permalink

https://escholarship.org/uc/item/7jq7g963

Journal

Proceedings of the National Academy of Sciences of the United States of America, 117(52)

ISSN

0027-8424

Authors

Hyon, Ryan
Youm, Yoosik
Kim, Junsol
et al.

Publication Date

2020-12-29

DOI

10.1073/pnas.2013606117

Peer reviewed

eScholarship.org Powered by the California Digital Library
University of California

Similarity in functional brain connectivity at rest predicts interpersonal closeness in the social network of an entire village

Ryan Hyon[a], Yoosik Youm[b,1], Junsol Kim[b], Jeanyung Chey[c], Seyul Kwak[d], and Carolyn Parkinson[a,e,1]

[a]Department of Psychology, University of California, Los Angeles, CA 90095; [b]Department of Sociology, Yonsei University, Seoul 03722, Republic of Korea; [c]Department of Psychology, Seoul National University, Seoul 08826, Republic of Korea; [d]Seoul Metropolitan Government – Seoul National University Boramae Medical Center, Seoul National University College of Medicine, Seoul 03080, Republic of Korea; and [e]Brain Research Institute, University of California, Los Angeles, CA 90095

Edited by Olaf Sporns, Indiana University, Bloomington, IN, and accepted by Editorial Board Member Michael S. Gazzaniga November 13, 2020 (received for review June 30, 2020)

People often have the intuition that they are similar to their friends, yet evidence for homophily (being friends with similar others) based on self-reported personality is inconsistent. Functional connectomes—patterns of spontaneous synchronization across the brain—are stable within individuals and predict how people tend to think and behave. Thus, they may capture interindividual variability in latent traits that are particularly similar among friends but that might elude self-report. Here, we examined interpersonal similarity in functional connectivity at rest—that is, in the absence of external stimuli—and tested if functional connectome similarity is associated with proximity in a real-world social network. The social network of a remote village was reconstructed; a subset of residents underwent functional magnetic resonance imaging. Similarity in functional connectomes was positively related to social network proximity, particularly in the default mode network. Controlling for similarities in demographic and personality data (the Big Five personality traits) yielded similar results. Thus, functional connectomes may capture latent interpersonal similarities between friends that are not fully captured by commonly used demographic or personality measures. The localization of these results suggests how friends may be particularly similar to one another. Additionally, geographic proximity moderated the relationship between neural similarity and social network proximity, suggesting that such associations are particularly strong among people who live particularly close to one another. These findings suggest that social connectivity is reflected in signatures of brain functional connectivity, consistent with the common intuition that friends share similarities that go beyond, for example, demographic similarities.

social networks | homophily | fMRI | resting state | functional connectomes

Human social networks exhibit a high degree of homophily, such that individuals who are close together in their social network (i.e., friends or friends of friends, rather than people further removed from one another in social ties) tend to be exceptionally similar to one another with respect to physical and demographic traits, such as age, gender, and ethnicity (1). Yet, a common intuition is that friends are similar to each other in ways that go beyond readily observable and relatively coarse characteristics, such as demographics. The most common method to assess such similarities is the administration of self-report surveys measuring how people tend to think and behave (i.e., personality). However, past research has found no evidence, or only relatively weak evidence, for a relationship between similarity in personality and social network proximity (e.g., refs. 2 and 3).

A separate body of research using functional MRI (fMRI) has shown that patterns of functional brain connectivity at rest comprise person-specific "fingerprints" that capture interindividual variability in a wide range of social, cognitive, and behavioral tendencies and capacities (4–10). These resting-state "functional connectomes" have also been shown to be predictive of individual differences in self-reported personality (11). Given that functional connectomes are predictive of an array of cognitive and behavioral phenotypes, interindividual similarities in functional connectomes may reflect similarities in how friends, and more generally people close to one another in their social network, think and behave. Such similarities may include those that are not sufficiently captured by widely used self-report surveys, such as measures of personality. Thus, fMRI can provide a window into the types of latent similarities that are associated with friendship. This approach is particularly promising given recent research integrating task-based fMRI and social network analysis, which has shown, for example, that when viewing videos, friends, and more generally, people closer together in their real-world social network, have exceptionally similar neural responses, which could be indicative of similarities in how friends attend to (12), understand (13), and interpret (14) the world (15, 16). Taken together with other recent work (17), these findings highlight the promise of integrating social network analysis and tools from cognitive neuroscience to improve our understanding of how individuals shape and are shaped by the real-world social networks in which they are embedded.

Significance

In what ways are we similar to our friends? Here, we characterized the social network of residents of a remote village, a subset of whom contributed personality and neuroimaging data. We demonstrate that similarity in individuals' resting-state functional connectomes predicts individuals' proximity in their real-world social network, even when controlling for demographic characteristics and self-reported personality traits. Our results suggest that patterns of functional brain activity during rest encode latent similarities (e.g., in terms of how people think and behave) that are associated with friendship. Taken together, integrating neuroimaging and social network analysis can offer novel insights into how the brain shapes or is shaped by the social networks that it inhabits.

Author contributions: R.H., Y.Y., J.K., J.C., S.K., and C.P. designed research; Y.Y., J.K., J.C., and S.K. performed research; R.H., Y.Y., J.K., and C.P. analyzed data; and R.H., Y.Y., and C.P. wrote the paper.

The authors declare no competing interest.

This article is a PNAS Direct Submission. O.S. is a guest editor invited by the Editorial Board.

Published under the PNAS license.

[1]To whom correspondence may be addressed. Email: yoosik@yonsei.ac.kr or cparkinson@ucla.edu.

This article contains supporting information online at https://www.pnas.org/lookup/suppl/doi:10.1073/pnas.2013606117/-/DCSupplemental.

First published December 14, 2020.

Here, we tested if patterns of neural responding at rest (e.g., individuals' functional connectomes) are associated with proximity between individuals in the social network of an entire village (Fig. 1). Specifically, we tested the hypothesis that greater similarity in individuals' functional connectomes would be associated with greater proximity between those individuals in the social network. Given the large body of research demonstrating that links between interpersonal similarity in a number of cognitive, affective, and behavioral outcomes and social network proximity disappear beyond three or four "degrees of separation" (18–26), we focused our analyses on people four or fewer "degrees of separation" from one another in the village's social network (*Materials and Methods*). We also tested if such relationships would persist after controlling not only for similarities in demographic characteristics but also for similarities in self-reported personality (i.e., the Big Five personality traits: extraversion, neuroticism, agreeableness, conscientiousness, and openness/intellect), which are thought to capture stable individual differences in people's cognitive, affective, and behavioral tendencies (27). Although self-report personality questionnaires capture much variation in how people tend to think and behave, there is considerable variance in such tendencies that is unaccounted for by such questionnaires (28) and that may be encoded in individuals' functional connectomes. Here, we tested if similarity in such latent traits is associated with proximity in a friendship network. Additionally, we examined which brain networks were particularly strongly associated with social network proximity to inform interpretations of the psychological significance of these results, as well as predictions for future research. Finally, given the well-established relationship between the physical distance between people and their distance from one another in social ties, we tested if geographic distance moderates the relationship between neural similarity and social network proximity.

Results

The complete social network of individuals living in a rural village community (29, 30) located on a South Korean island consisting primarily of older adults was characterized (Fig. 1). The relative homogeneity of this sample with respect to demographic characteristics, such as age and race (*Materials and Methods*), facilitates testing hypotheses regarding relationships between neural similarity and social network proximity, above and beyond interindividual similarity in demographic variables (which were further accounted for in all statistical analyses). A subset of individuals who participated in the social network survey also participated in the fMRI study, in which they underwent resting-state fMRI. Within each connected component of the social network, the social network proximity between every unique pair of fMRI participants was calculated; data from pairs of participants within all connected components were combined for statistical analyses (Fig. 1; see *Materials and Methods* for further details). We then characterized each fMRI subject's whole-brain resting-state functional connectome (Fig. 2*A* and *Materials and Methods*). Intersubject similarities in functional connectomes were then calculated, and the resulting dyadic connectome similarity vectors were subsequently used to predict individuals' social network proximity (Fig. 2*B* and *Materials and Methods*). We also tested for relationships between social network proximity and similarity in connectivity within and between functional brain networks (*Materials and Methods*).

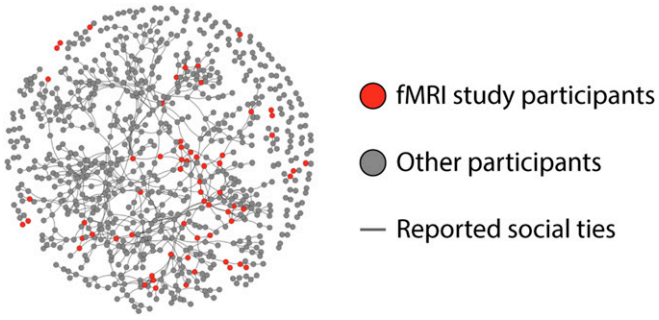

Fig. 1. Social network characterization. Residents of a rural village located on a small island completed a survey in which they indicated their social ties with other individuals in their community. The complete social network (n = 798) of the village was reconstructed using this data, and a subset of residents (red nodes; n = 64) participated in the fMRI study. Lines ("edges") indicate the existence of a reciprocated or unreciprocated social tie between individuals. For visualization purposes, unweighted edges were used to depict social ties. However, in our analyses, edges were weighted by individuals' ratings of emotional closeness with one another (*Materials and Methods*).

Intersubject Similarity in Neural Activity Predicts Social Network Proximity in the Absence of a Stimulus. We first implemented a data-driven, machine-learning approach to predict social network proximity based on intersubject similarities in multivariate patterns of resting-state functional connectivity distributed across the entire brain using a partial least squares regression (PLSR)-based algorithm (see *Materials and Methods* for further details). Using a 10-fold cross-validation scheme, the algorithm significantly predicted individuals' social network proximity based on the similarity in their functional connectomes, such that the actual proximity between individuals in the social network was significantly correlated with what was predicted by the model ($r = 0.502$, $P = 1.322 \times 10^{-15}$), while controlling for their similarities in demographic variables, such as age and gender (Fig. 3*A*). Given the dependency structure of the data (i.e., the same individual participates in multiple dyads), we conducted permutation testing to more conservatively estimate the significance of the correlation between real and predicted social network proximity values across dyads (see *Materials and Methods* for further details). As shown in Fig. 3*B*, the true r value was significantly greater than the majority of the 5,000 permuted r values ($P = 0.036$).

Through the algorithm's dimension reduction procedure (*Materials and Methods*), 293 unique neural similarity predictors were consistently selected across all 10 cross-validation data folds to be used in predicting social network proximity (see *Materials and Methods* for further details). As shown in Fig. 3*C*, these predictors measured intersubject similarity in functional connectivity within and between several networks, and predictors associated with the default-mode network (DMN) were most frequently selected by the algorithm. The consistently selected predictors, as well as the locations of the most frequently implicated nodes (e.g., in left ventrolateral prefrontal cortex, the left inferior parietal lobule, and left medial prefrontal cortex), are also visualized on "glass brain" models in *SI Appendix*, Fig. S1. However, given the large number of consistently selected predictors, chord diagrams are provided to convey information about the implicated brain networks (Fig. 3). Similar results were observed when repeating this analytic procedure excluding dyads that live in the same residences ($p_{permutation} = 0.039$; *SI Appendix*, Fig. S2), such that similarity in functional connectomes significantly predicted social network proximity and predictors associated with the DMN were most frequently selected by the algorithm. Similar results were also observed when weighting edges by the frequency with which individuals communicate with each other ($p_{permutation} = 0.013$; *SI Appendix*, Fig. S3) or the frequency with which they meet with each other ($p_{permutation} = 0.002$; *SI Appendix*, Fig. S4), rather than weighting edges by emotional closeness ratings. Functional connectome similarity was not, however, predictive of social network proximity when

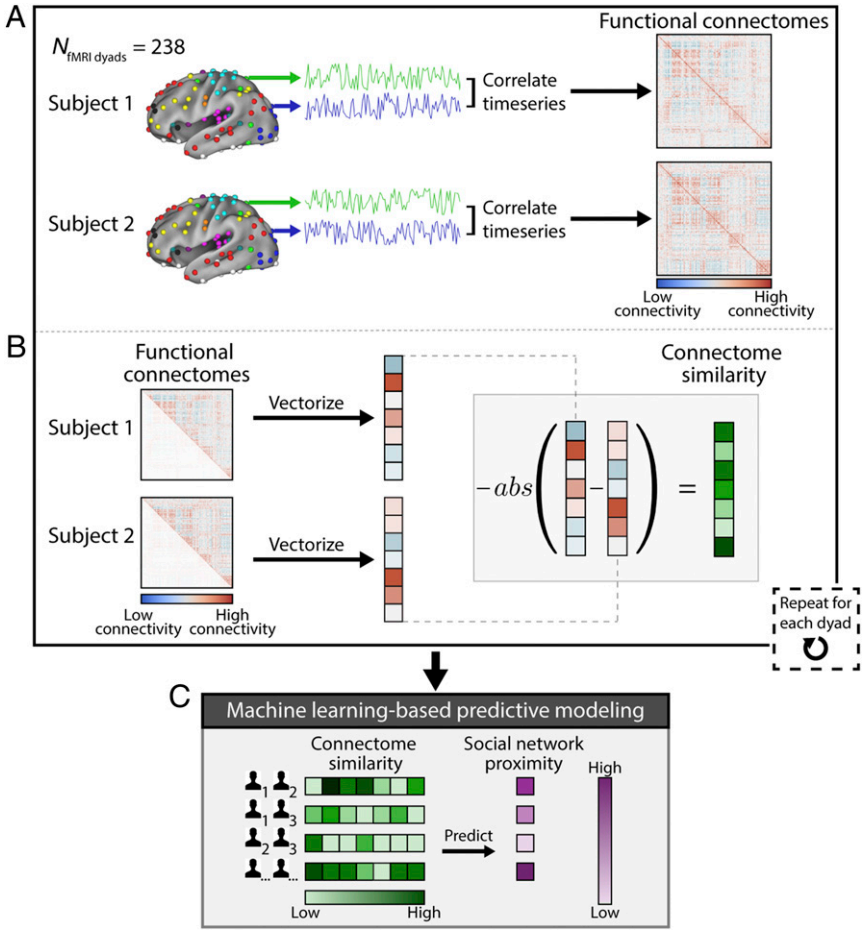

Fig. 2. Functional connectome-based predictive modeling of social network proximity. (*A*) Subjects' data were resampled to standard space, and the Power et al. (31) atlas was used to define ROIs. Each ROI is associated with 1 of 13 functionally defined brain networks, signified by different colors. For each fMRI subject, we then calculated pairwise Pearson correlations between neural time series extracted from a 15-mm-radius sphere centered on each ROI to form a functional connectivity matrix (i.e., a functional connectome). (*B*) The off-diagonal elements in the upper triangular half of each subject's functional connectome were then flattened into a vector. For each unique pair of fMRI subjects, intersubject similarity in their connectome vectors was measured by calculating pairwise Euclidean distances between corresponding functional connectivity values in subjects' respective connectome vectors. (*C*) We used a partial least-squares regression-based algorithm to predict individuals' social network proximity based on the similarity in their functional connectomes (see *Materials and Methods* for further details).

computing social distance in the social network without incorporating edge weights that encode relative interpersonal closeness for directly connected dyads (i.e., emotional closeness, communication frequency, and meeting frequency), as shown in *SI Appendix*, Fig. S5.

Individuals Who Are Close Together in Their Social Network Share Similar Functional Connectomes. In an exploratory analysis, we assessed the direction of the linear relationship between social network proximity and each of the neural similarity predictors selected across all cross-validation data folds to determine if social network proximity was positively associated with similarity in functional connectivity (see *Materials and Methods* for further details). Indeed, 261 of the 293 predictors (89%) were positively associated with social network proximity (Fig. 3*D*); the remaining 32 predictors were negatively associated with social network proximity (Fig. 3*E*).

Individuals Who Are Close Together in Their Social Network Share Similar Functional Connectivity within and between Brain Networks. To complement our data-driven predictive modeling analysis and better inform interpretation of the types of neural similarity associated with social network proximity, we tested if social network proximity was associated with intersubject similarity in functional connectivity within and between each of the 13 functional brain networks defined in the Power et al. (31) atlas. For each of the 91 statistical tests (13 tests based on within-network connectivity similarity; 78 tests based on between-network connectivity similarity), we adapted the method outlined by Chen et al. (32) to fit linear mixed-effects models with crossed random effects to account for the dependency structure of the data (*Materials and Methods*).

Similarity in functional connectivity was significantly associated with social network proximity when controlling for demographic similarities in nine of these models (Table 1). In all nine models, we observed a positive relationship between functional connectivity similarity and social network proximity, indicating that in cases where the relationship between social network proximity and neural similarity was significant, greater neural similarity was associated with greater proximity in the social network. These effects remained statistically significant after correcting for multiple comparisons across 91 statistical tests using false discovery rate (FDR) thresholding, as shown in Table 1. Consistent with the results of the predictive modeling

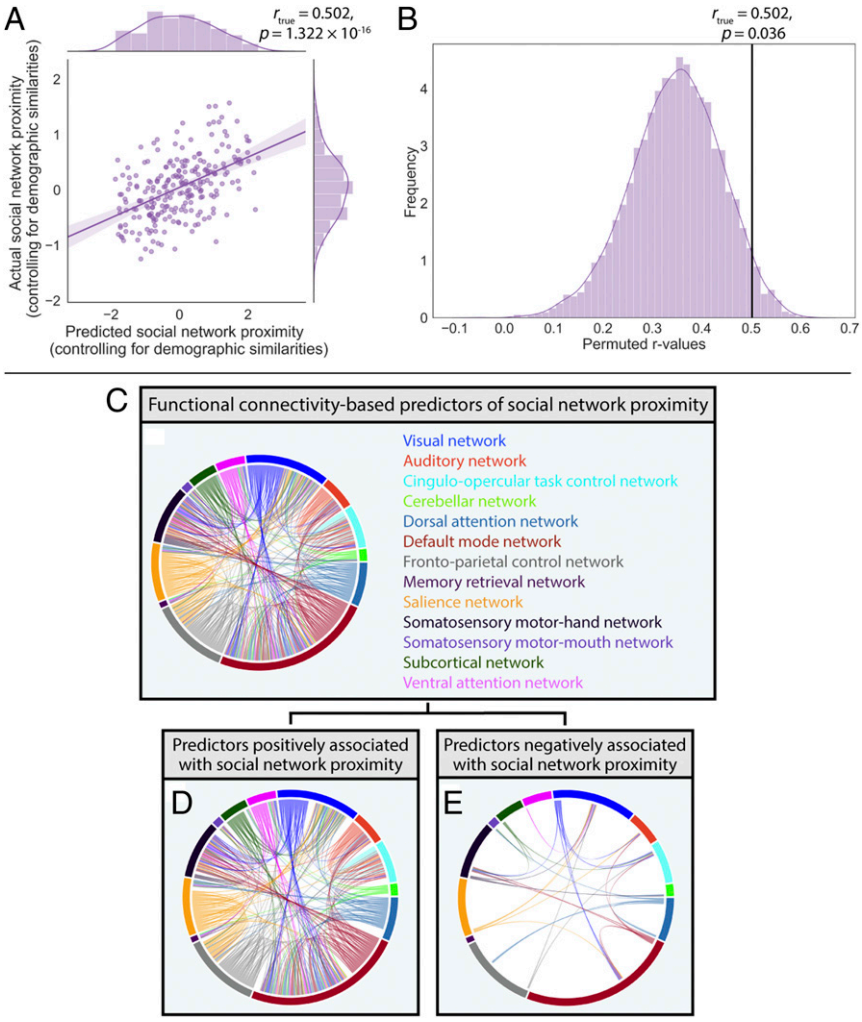

Fig. 3. Intersubject similarity in functional connectomes predicts social network proximity. (*A*) The PLSR-based algorithm successfully predicted social network proximity from left-out data while controlling for intersubject similarities in demographic variables. The algorithm's predicted social network proximity was significantly associated with actual social network proximity. (*B*) This relationship was significant after conducting permutation testing to account for the dependency structure of the data (see *Materials and Methods* for further details). (*C*) The algorithm consistently selected a multivariate pattern that included 293 neural similarity predictors across all 10 cross-validation data folds for predicting social network proximity. These predictors spanned all 13 functional brain networks defined in the Power et al. (31) atlas. (*D*) A positive relationship between 261 of these 293 predictors and social network proximity was observed. (*E*) In contrast, only 32 predictors were negatively associated with social network proximity. Note: Colors used for connections between two different brain networks were arbitrarily assigned to one of the two implicated networks.

analyses, the connectivity of areas in the DMN was particularly frequently linked to social network proximity; three of the nine models in which social network proximity was significantly linked to neural similarity involved the DMN (Table 1). Similar results were observed when repeating this analytic procedure excluding cohabitating dyads (*SI Appendix*, Table S1) and when weighting social ties by interindividual communication frequency (*SI Appendix*, Table S2) or by meeting frequency (*SI Appendix*, Table S3) rather than by interpersonal closeness, as well as when social ties were unweighted (*SI Appendix*, Table S4).

Intersubject Similarity in Functional Connectomes Was Associated with Social Network Proximity while Controlling for Personality Similarity. In additional exploratory analyses, the same data analytic procedures described above were repeated to test if social network proximity is associated with similarity in functional brain connectivity while controlling not only for demographic similarities but also for similarities in self-reported personality traits.

In the predictive modeling analysis, the algorithm successfully predicted individuals' proximity to one another in the social network based on the similarity of their functional connectomes while controlling for similarities in the Big Five personality traits and demographic variables ($r = 0.477$, $P = 6.795 \times 10^{-15}$). This significant relationship between actual and predicted social network proximity remained significant after implementing permutation testing to account for the dependency structure of the data ($P = 0.048$). The algorithm's dimension reduction procedure yielded a set of neural similarity predictors that were remarkably similar to those reported in the primary predictive modeling analysis, which controlled only for intersubject similarities in demographic variables. Similarly, there was an overwhelmingly positive relationship between these predictors and social network proximity (*SI Appendix*, Fig. S6).

We also tested if, when controlling for interindividual similarity in the Big Five personality traits, social network proximity would remain significantly positively related to neural similarity when using linear mixed-effects models to characterize similarity in functional connectivity within and between functional brain networks. As in our main analyses using this approach, social network proximity was associated with similarity in functional

Table 1. Results of linear mixed-effects models testing for associations between functional connectivity within and between brain networks and social network proximity

Brain network(s)	β	SE	P	P (FDR-corrected)
DMN-VAN	0.183	0.068	1.803×10^{-4}	0.016
DMN-CN	0.165	0.067	0.001	0.017
SMHN-SMMN	0.165	0.066	4.807×10^{-4}	0.017
DMN-DAN	0.164	0.068	0.001	0.018
COCN	0.160	0.068	0.001	0.018
FPCN-SAN	0.164	0.071	0.001	0.018
AN-SMHN	0.150	0.067	0.002	0.022
DMN-FPCN	0.147	0.067	0.002	0.026
COCN-AN	0.151	0.071	0.003	0.029

Each model included crossed random effects for participants and a fixed effect for neural similarity, with social network proximity as the outcome variable. P values and SEs were adjusted to account for data redundancy (*Materials and Methods*). Only significant associations are shown. AN, auditory network; CN, cerebellar network; COCN, cingulo-opercular task control network; DMN, default mode network; DAN, dorsal attention network; FPCN, frontoparietal task control network; SAN, salience network; SMHN, somatosensory motor-hand network; SMMN, somatosensory motor-mouth network; VAN, ventral attention network.

connectivity between several pairs of brain networks after accounting for personality similarity. Again, all significant relationships were positive (i.e., greater social network proximity was associated with greater neural similarity in all cases). As in the main results, when accounting for both demographic and personality similarity, the DMN appeared most frequently in the models in which social network proximity was associated with similarity in functional connectivity within and between brain networks (*SI Appendix*, Table S5).

For both sets of analyses (i.e., both for predictive modeling analyses and for analyses measuring relationships between social network proximity and similarity in functional connectivity within and between brain networks using linear mixed-effects models), when controlling for similarity in the Big Five personality traits convergent results were obtained when defining the social network in different ways. For example, similar results were obtained when excluding dyads composed of members who live in the same residences both when using predictive modeling ($p_{permutation}$ = 0.026; *SI Appendix*, Fig. S7) and linear mixed-effects models (*SI Appendix*, Table S6) and when social ties were weighted by interindividual communication frequency (see *SI Appendix*, Fig. S8 for predictive modeling results, $p_{permutation}$ = 0.039; see *SI Appendix*, Table S7 for results using linear mixed-effects models) or by meeting frequency (see *SI Appendix*, Fig. S9, $p_{permutation}$ = 0.011, and *SI Appendix*, Table S8), rather than by emotional closeness. Using a social network in which edges were unweighted (i.e., in which emotional closeness and frequency of communication or meeting were not considered), neural similarity was not predictive of social network proximity using our predictive modeling approach (as in the main results; see *SI Appendix*, Fig. S10); however, neural similarity remained positively associated with proximity in the social network using linear mixed-effects models based on similarity in connectivity within and between functional brain networks (as in the main results; see *SI Appendix*, Table S9). Taken together, these results suggest that intersubject similarity in functional connectomes is associated with social network proximity, particularly when taking into account information about the relative interpersonal closeness of directly connected dyads (e.g., emotional closeness, communication frequency, and meeting frequency). Furthermore, these relationships are not due to interpersonal similarity in terms of the personality traits measured here (i.e., the Big Five personality traits).

Connectome Similarity Is Most Strongly Related to Social Network Proximity among Individuals Who Live Close to One Another. The results of our primary analyses demonstrate that similarity in individuals' functional connectomes is associated with proximity in their real-world social network. Prior work has also established a relationship between geographic proximity and social network proximity (33–35). We explored if and how geographic proximity might impact the relationship between neural similarity and social network proximity.

Very similar people who live far from one another may be less likely to become friends (compared to very similar people who live close to one another), as greater physical distance could lead to fewer encounters. Living close by may provide opportunities for people to befriend those with whom they are especially compatible (including, for example, similar others). In the same vein, associations between neural similarity and social network proximity may also be particularly pronounced among people who live close to one another if such associations reflect social influence (i.e., social network proximity causing similarity), rather than, or in addition to, assortativity (i.e., similarity causing social network proximity). For example, there may be more opportunities for interpersonal influence effects to unfold among people who are close to one another in both social ties and their physical location. Both of the possibilities described above would predict that the relationship between neural similarity and social network proximity would be strongest among people in close geographic proximity to one another. It is also possible that neural similarity would be most strongly related to social network proximity among people who live relatively far from one another—for example, people may only maintain friendships with those who live far from themselves if they are exceptionally compatible with one another.

To begin to arbitrate between these possibilities, we conducted an additional exploratory analysis to test whether geographic distance moderates the relationship between connectome similarity and social network proximity. To calculate a single variable measuring intersubject similarity in functional connectomes that approximated the neural similarity data used in the predictive modeling analysis, we used the aforementioned PLSR-based algorithm and extracted the primary PLS component (*Materials and Methods*). A linear mixed-effects model with crossed random effects for both participants was used to test for an interaction between the effects of connectome similarity and geographic distance on social network proximity; the main effects of geographic distance and neural similarity were also included in the model (*Materials and Methods*). We note that the results of the analyses reported in the preceding sections should be used to assess relationships between neural similarity and social network proximity; the purpose of this analysis was specifically to test if and how geographic distance moderates the relationships between connectome similarity and social network proximity reported above.

We observed a significant interaction between geographic distance and neural similarity (β = −0.163, SE = 0.044, P < 0.0001); significant main effects of neural similarity (β = 0.840, SE = 0.071, P < 0.0001) and geographic distance (β = −0.322, SE = 0.066, P < 0.0001) were also observed. The main effect of geographic distance suggests that people who lived closer to one another in the village tended to be closer to one another in the social network. To better understand the interaction between neural similarity and geographic distance, we conducted a simple slopes analysis. This revealed significant associations between neural similarity and social network proximity among people who lived close to one another in the village (i.e., for whom the walking distance between dyad members' residences was

approximately one SD below the mean; see *Materials and Methods*), $\beta = 0.994$, 95% CI [0.835, 1.154], SE = 0.081, $t = 17.280$, $P < 0.0001$, as well as among people who lived an average distance from one another in the village, $\beta = 0.839$, 95% CI [0.702, 0.976], SE = 0.070, $t = 16.963$, $P < 0.0001$, and among people who lived far from one another in the village (i.e., walking distance one SD above the mean), $\beta = 0.677$, 95% CI [0.513, 0.839], SE = 0.083, $t = 11.480$, $P < 0.0001$. Thus, the relationship between neural similarity and social network proximity appeared to be most pronounced among those who lived closest to one another in the village (Fig. 4).

We also observed a significant interaction between the effects of neural similarity and geographic distance on social network proximity in four of the nine models in which similarity in functional connectivity within and between brain networks was associated with social network proximity. This is consistent with the notion that the relationship between connectome similarity and social network proximity is contingent on geographic proximity (*SI Appendix*, Fig. S11). As in the moderation analysis using the primary PLS component described above, in three of these four models the most positive relationship between neural similarity and social network proximity was observed among participants who lived closest to one another—specifically, this was the case in models characterizing similarity in connectivity 1) between the DMN and the dorsal attention network, 2) between the DMN and the frontoparietal task control network, and 3) within the cingulo-opercular task control network. That said, there was some heterogeneity in the nature of this interaction across models. For example, in the remaining model that evinced a significant interaction, the strongest relationship between neural similarity and social network proximity was observed among people whose homes were relatively far apart (*SI Appendix*, Fig. S11). As such, we hesitate to draw strong conclusions from these exploratory moderation analyses. In order to move toward a more systematic understanding of these phenomena, we suggest that future work continue to investigate how interpersonal similarity and geographic proximity interact to predict social network proximity.

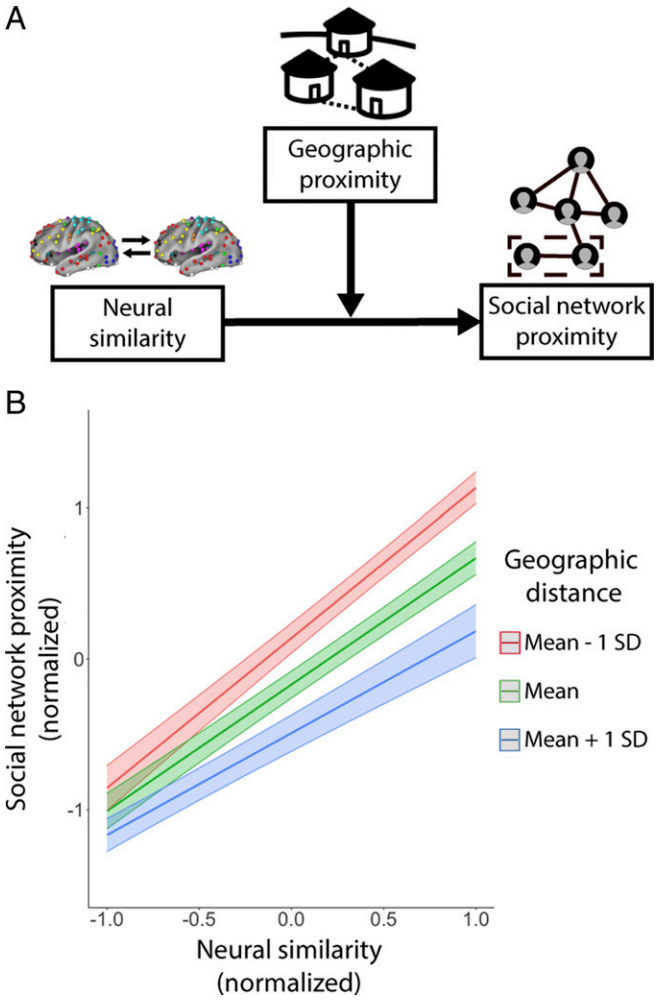

Fig. 4. Geographic proximity moderates the relationship between connectome similarity and social network proximity. (*A*) We tested if geographic distance moderates the relationship between neural similarity and social network proximity. (*B*) A linear mixed-effects model was used to test for an interaction between the effects of connectome similarity and geographic distance on social network proximity (*Materials and Methods*). We observed a significant interaction between geographic distance and connectome similarity, such that the relationship between neural similarity and social network proximity was especially pronounced among individuals who lived closest to one another in the village (*Results*). Shaded areas represent 95% confidence intervals.

Discussion

The current results demonstrate that similarity in individuals' patterns of neural connectivity at rest is related to closeness in their real-world social network, above and beyond effects of demographic variables or the Big Five personality traits. These findings are in line with past research showing that friends exhibit similar neural responses when perceiving naturalistic stimuli (e.g., movies), which have been attributed to similarities in how people close together in social ties interpret and respond to their environment (15, 16). The current findings demonstrate that friendship and social network proximity are related not only to individuals' neural responses to exogenous stimuli but also to their intrinsically organized neural activity at rest. Prior work has demonstrated that an individual's whole-brain resting-state functional connectome can function as a "fingerprint," in that it is both uniquely identifying and stable across disparate points in time (5, 36). Here, we show that intersubject similarity in a distributed pattern of functional connectivity is associated with social network proximity. Similarity in individuals' connectomes was overwhelmingly positively associated with their social closeness in the real world, suggesting that friends share similar resting-state activity. Moreover, we find that the relationship between connectome similarity and social network proximity is moderated by physical proximity, such that the link between neural similarity and social network proximity tends to be most pronounced among people who live close to one another. Integrating the current findings into the extant literature on resting-state functional connectivity can shed light on the types of individual difference variables that may be exceptionally similar among friends and inform hypotheses to test in future research, as described in more detail below.

We found that similarity in functional connectivity at rest was associated with social network proximity while controlling for demographic similarities. We also observed remarkably similar results while controlling for intersubject similarity not only in demographic variables but also in the Big Five personality traits. Despite recent evidence demonstrating that similarity in functional connectomes is associated with similarity in the Big Five personality traits (37), personality data do not account for the current results, in which similarity in functional connectomes was associated with friendship above and beyond the effects of similarity in the Big Five personality traits. Rather, the aspects of functional connectome similarity that predicted friendship in the current study may be related to similarities in latent cognitive, emotional, and/or behavioral traits that are exceptionally similar among friends but that are not sufficiently captured by the

self-report personality measure used here. When considered in tandem with the current results, the large body of research linking cognitive, emotional, and behavioral variables to functional brain connectivity (38) provides preliminary clues regarding what kinds of interpersonal similarities might underlie the observed relationship between neural similarity and social network proximity. For example, patterns of resting-state connectivity associated with the frontoparietal task control and somatomotor networks have recently been shown to be predictive of individual differences in trait empathic concern (10). Similarly, functional connectivity of the DMN is predictive of a component of empathy reflecting the extent to which an individual feels another's pain (39). Variables that are not traditionally considered social may also underlie relationships between neural similarity and social network proximity. For example, past work demonstrates that people close together in a social network have particularly similar neural responses in regions associated with attentional allocation, such as the superior parietal lobule, while viewing movies (15, 16). Interindividual similarity in attentional allocation, and in other processes that are not inherently social, could facilitate the development of a sense of "generalized shared reality" (i.e., the sense of sharing similar thoughts, feelings or beliefs with someone else, including about the world outside of one's social relationships or interactions), which has recently been shown to predict social connection between individuals (40). Thus, past work linking resting-state connectivity within and between the brain networks implicated in the current study to individual difference variables that are not typically considered "social" may also be relevant. For example, functional connectivity of the DMN has been linked to individual differences in creativity (7), memory (6), fluid intelligence (25), and attentional skills (41). In the current study's predictive modeling analysis, of the functional connectivity-based predictors that best predicted social network proximity, 45% were associated with the DMN; moreover, in the analyses linking connectivity within and between specific brain networks to social network proximity the DMN was the most frequently implicated network. Thus, the current results point to testable hypotheses about the kinds of interpersonal similarities that may be particularly pronounced among people close to one another in social ties. These interpersonal similarities may include similarities in social characteristics (e.g., different facets of empathy) and in qualities that are typically not considered social but that might have implications for social connection to the extent that they are similar or dissimilar across individuals.

While the current study was primarily concerned with testing if individuals' social network proximity was linked to the similarity of their functional connectomes, we also conducted an exploratory analysis testing if geographic distance moderates this relationship, given the well-established link between individuals' physical closeness and social closeness in the real world (42–45). Associations between similarity in functional connectivity and social network proximity appeared to be strongest among people who lived close to each other in the village (Fig. 4). This could plausibly be caused by the constraints that geographic distance can impose on both assortativity and social influence processes. For example, assortativity may unfold more readily among people who live close to one another than among people who live far apart, given that similar people who live far from one another may be less likely to meet and befriend one another than similar people who live close to each other. On the other hand, social influence processes may unfold most readily among people who are close to one another in both social ties and physical space.

More generally, the current results alone are unable to inform claims about the causal relationship between functional connectome similarity and social network proximity. As noted above, the moderating role of geographic distance could plausibly stem from assortativity or social influence processes. Future longitudinal studies should test if preexisting similarities in resting-state activity causally predict social network proximity or if social network proximity facilitates the convergence of individuals' functional connectomes over time. For example, preexisting similarities in functional connectomes that reflect latent trait similarities may foster friendship formation due to interpersonal similarities facilitating communication and affiliative tie formation (46, 47). This would be consistent with suggestions that misattunement between individuals disrupts the smoothness of social interactions (48) and may account for some instances of social disconnection, including, but not limited to, the social disconnection that characterizes some forms of psychopathology—that is, with the "social interaction mismatch hypothesis" (48, 49). Future work could test this possibility by combining the forms of data collected in the current study with unobtrusive behavioral measures of interpersonal coordination and orienting during social interactions (50).

Alternatively, the current findings could stem from well-established social influence processes that unfold within dyads (51, 52) and percolate outward in social networks, causing people to influence and be influenced by others to whom they are connected only indirectly (42). Future work could use unobtrusive methods to track interaction patterns between individuals (53) and how people approach and attend to one another during interactions (50) to enrich understanding of how social influence effects unfold over time in the real world. The repeated, intensive, and sustained interactions that characterize friendships may lead friends to develop similarities in how they tend to think, feel, and behave, which become entrenched over time and reflected in patterns of brain connectivity. In other words, in the same way that sustained and intensive practice on complex cognitive tasks involves particular patterns of engagement of specific brain networks that impact future characteristics of functional connectivity at rest (54), sustained and intensive interactions between friends could lead to convergence in styles of thinking, feeling, and behaving that are reflected in similarity in functional brain connectivity at rest. Living near one's friends may make it easier to have intensive and frequent interactions with them, which in turn could foster greater interpersonal similarity over time. This would be consistent with the findings that connectome similarity was most strongly associated with social network proximity among people who lived close to one another (Fig. 4) and that connectome similarity was particularly predictive of social network proximity when weighting edges in the social network by in-person meeting frequency (*SI Appendix*, Fig. S4). It is also possible that assortativity and social influence processes interact; for example, social network proximity may increase interpersonal similarity through social influence, and the resultant interpersonal similarities may further promote friendship formation [e.g., because interpersonal similarity increases the predictability of social interactions, leading to more fluid and enjoyable interactions, and thus increasing the likelihood of friendship formation (46)]. Future work using longitudinal designs will be important to elucidate the relative contributions of these mechanisms to the correspondence between similarity in patterns of neural responding at rest and social network proximity.

The unique characteristics of our sample should be taken into consideration when interpreting the current results. Given that our sample consists of older adults living in a remote, rural village on an island in South Korea, future work should test whether functional connectomes are predictive of social network proximity in additional samples. Similarly, future work should investigate whether the neural variables important for predicting social network proximity in the current study are also important for predicting social network structure in other communities. The kinds of interpersonal similarities that engender or result from social network proximity likely vary across contexts, and

thus investigations involving different communities (e.g., communities in different cultural settings and different age groups) may yield different results (55). In a similar vein, the magnitude of the relationship between geographic distance and social network proximity, as well as the interaction between geographic distance and interpersonal similarity in predicting social network proximity, likely differs across contexts (e.g., depending on an area's population density and the extent to which geographic and functional distance are associated in a given community). Furthermore, given prior work demonstrating that similarity in neural responses to naturalistic stimuli is also predictive of social network proximity (15, 16) and that tasks can emphasize individual differences in functional connectivity (56), future work should test if and how interpersonal similarity in functional connectivity during tasks, including naturalistic stimulation, is associated with social network proximity. Relatedly, future work could examine how social network proximity relates to similarity in neural responding in social contexts, given recent evidence that social network variables relate to differential patterns of neural responding in social contexts, such as when making recommendations to others (57) or experiencing social exclusion (58). Similarly, in light of past work demonstrating that neural synchrony is associated with successful communication (59), future work could benefit from considering how functional connectivity during social interactions relates to the quality of those interactions, and more generally, from adopting a "second-person neuroscience" approach to examine neural processes during real-time social interactions (60). Additionally, given that some forms of interpersonal misattunement (e.g., diverging prediction and interaction styles) may disrupt social interactions and the formation of social connections in several psychiatric conditions (48, 49, 60), future work could examine how idiosyncratic patterns of functional connectivity relate to social impairments that characterize many forms of psychopathology (49) and social disconnection more generally (61).

Taken together, the current results suggest the possibility of homophily based on similarities in neural responding at rest. More specifically, we find that similar patterns of resting-state functional connectivity distributed across the brain are associated with friendship and social network proximity. Past research on homophily has often focused on relatively coarse variables, such as demographic characteristics; prior work testing the relationship between friendship and similarities in personality has tended to yield null or inconsistent patterns of findings. Thus, much remains unknown regarding how friendship and social network proximity relate to interindividual similarities in psychologically meaningful variables. However, the current study suggests that similarities in functional connectomes may capture similarities in meaningful latent variables that are distinct from demographic characteristics and the Big Five personality traits and that are associated with individuals' social closeness in their real-world social network. Thus, functional connectomes could serve as neural signatures that identify individuals who are likely to form social ties and, more generally, as powerful tools for studying how individuals' brains influence, and are influenced by, the structure of real-world social networks.

Materials and Methods

Part 1: Social Network Characterization.

Subjects. Individuals in Part 1 of the study were subjects from the third wave of the Korean Social Life, Health, and Aging Project [KSHAP (30, 62)]. KSHAP is a study on the health and social networks of older adults in rural communities in South Korea. The current sample of subjects reside in Township K, Ganghwa-gun in South Korea, and the size of the township is 26.43 km^2. The total township population was 860 individuals, and 591 individuals (349 females, mean age = 72.79, SD = 7.18) participated in the social network survey, resulting in a response rate of 68.7%. The study was approved by and performed in accordance with the standards of the Institutional Review Board of Yonsei University, and all subjects provided written informed consent for the experiment. See ref. 30 for a comprehensive overview of measures included in Wave 1 of KSHAP data collection. In addition to the measures listed in ref. 30, the third wave of KSHAP data included resting state fMRI data on a subset of participants, as well as additional measures of general cognitive functioning (used for screening fMRI participants as described in *Subjects*) and a measure of personality [the Big Five 44-item Inventory (63)].

Social network characterization. The social network survey was administered in the subjects' homes and in community centers. Subjects responded to a survey asking them to enumerate their social network members ("alters"), including a spouse (if any) and up to five people with whom they most often discussed important concerns in the past 12 mo. This first prompt read, "People often discuss important things with others. For example, this could be something good or bad that happened to you, or it could be your usual worry. When you look back over the past year, how many people do you talk to often about important things, and who are those people?" In a second prompt, subjects were also asked to enumerate a "very important" seventh individual. This second prompt read, "Is there any person who seems very important to you, other than your spouse or the discussion partners whom you mentioned? This person would be someone with whom you have not been in frequent discussions over the past year, but with whom you are still feeling friendly." These "very important" alters were not included in subsequent data analysis given that the nature of these alters is qualitatively different from those enumerated in response to the first prompt. Subjects provided information about each alter's name, gender, and residence. Subjects were also asked to rate the extent to which they were emotionally close with each of their alters (1: Not very close; 2: Somewhat close; 3: Very close; 4: Extremely close). Alters who were not married to the subjects and living outside of Township K were excluded. Alters who were enumerated by more than one subject were identified based on the following criteria: 1) At least two out of three Korean characters in their names matched, 2) their gender matched, 3) their age difference was less than 5 y, and 4) their addresses belonged to the same village.

Social network analysis was performed using the Python package igraph (64). We constructed a weighted, undirected graph, in which at least one social tie between two nodes (i.e., nomination) was sufficient to constitute an undirected edge. For example, an undirected edge would connect two nodes, $person_i$ and $person_j$, if 1) $person_i$ nominated $person_j$ as an alter, 2) $person_i$ nominated $person_i$ as an alter, or 3) $person_i$ and $person_j$ each nominated the other as an alter. For reciprocated edges ($n = 270$), each edge was weighted by the mean of emotional closeness ratings provided by each member of the dyad. For unreciprocated (i.e., not mutually reported) ties ($n = 745$), if both dyad members had completed the survey, the corresponding single emotional closeness rating was averaged with 0 (i.e., divided by 2) in order to account for the unreciprocated nature of nonmutual social ties. The resultant penalized emotional closeness value was used to weight the undirected edge. However, in cases where the nominated alter would have been incapable of reciprocating the nomination (i.e., in cases where the alter did not participate in the survey; $n = 320$ edges), the corresponding single emotional closeness rating was used to weight the undirected edge. The resulting social network graph consisted of a total of 799 nodes and 1,015 edges and was used to estimate social distances between individuals.

Our main analyses involved weighting edges by ratings of emotional closeness. As mentioned in *Results* (see *SI Appendix* for further details), we repeated our main analyses using networks in which edges were 1) weighted by communication frequency, 2) weighted by meeting frequency, and 3) unweighted. While communication and meeting frequencies were highly correlated with one another ($r = 0.90$), correlations between emotional closeness ratings and meeting frequency ($r = 0.28$) and between emotional closeness ratings and communication frequency ($r = 0.32$) were comparatively modest.

Social distances were computed between fMRI participants within each connected component of the social network (Fig. 1); data from dyads within all connected components of the social network were concatenated for subsequent statistical analyses. For our main analyses, and for additional analyses using alternative edge weightings, Dijkstra's algorithm (65) was used to calculate the social distance between members of dyads within each connected component. Dijkstra's algorithm finds the path of "least resistance" between each pair of nodes, where "resistance" is defined as the cost of traversing a path between those nodes; here, cost was defined as the inverse of an edge's weight. Thus, weighted social distance was defined as the smallest sum of inverted edge weights across intermediary edges between two individuals. Alternatively, social distance can be operationalized as the smallest number of intermediary edges required to connect two individuals in the network (i.e., geodesic distance), where all edges are

weighted equally. As noted above, social distances based on edges weighted by emotional closeness, which were highly correlated with unweighted social distances ($r = 0.88$), were used for our main analyses so that emotional closeness could be taken into account. We then negated the weighted social distance values to convert them into social network proximity values (i.e., higher values reflect greater closeness in the social network) in subsequent analyses.

Part 2: Neuroimaging Study.

Subjects. Of the 591 individuals that participated in Part 1, 195 individuals underwent further screening for preclinical neurocognitive disorders 1 y later. Individuals were excluded if they 1) scored 1.5 SD below the mean on the Mini-Mental State Examination for Dementia Screening (66), 2) were in the fifth percentile on the Long-term Memory Recall Index or Working Memory Index in the Elderly Memory Scale (67), or 3) had significant cognitive or behavioral changes in the preceding year, as assessed using the Clinical Dementia Rating (68). Sixty-eight subjects passed the screening process and participated in the fMRI session, in which they were instructed to rest quietly with their eyes open and not to fall asleep. Three subjects were excluded due to excessive movement, neurological abnormality, and diffuse signal confounds. One subject did not complete the social network survey and was also excluded.

Of the remaining 64 fMRI subjects, there were 2,016 unique potential fMRI dyads. Of the 2,016 unique fMRI dyads, 737 dyads had undefined distances between them (i.e., nodes were in separate components of the network) and were excluded from analysis. Of the 1,279 remaining dyads, 1,038 dyads were characterized by a geodesic distance greater than four and were excluded from analyses given prior work demonstrating that similarities in neural responses in people four or more "degrees of separation" apart are highly variable and not significantly different from that of social dyads two or three "degrees of separation" from one another (15). More generally, a large body of research demonstrates that relationships between interpersonal similarities in a variety of cognitive, emotional, and behavioral phenomena (e.g., risk perception, cooperation, smoking, depression, loneliness, and happiness) and social network proximity disappear beyond three to four "degrees of separation" (18–24). This widely documented phenomenon may result from social influence effects decaying with social distance (69), the relative instability of long chains of social ties (69), assortativity (i.e., attraction to similar others) only being possible when opportunities to encounter similar others exist (which becomes less likely as individuals become further removed from one another in social ties), or some combination of these factors. While the current work does not attempt to arbitrate between these possibilities, we limited our analyses to dyads four or fewer "degrees of separation" from one another in light of these findings.

We note that recoding very large social distances to a common value (e.g., ~4) would have minimal impact when analyzing networks with smaller diameters and fewer dyads at remote social distances from one another (e.g., when analyzing the social network of a classroom rather than a village, city, or province). However, in networks with larger diameters (here, the diameter of the largest connected component in the network is 18) and where the vast majority of dyads have a social distance greater than four (here, 1,038 out of 1279, or 81% of fMRI dyads), recoding high social distance dyads would result in the vast majority of dyads being assigned the same social distance value (e.g., of four). Moreover, because we hypothesize that this very large set of dyads would be extremely heterogeneous with respect to their level of similarity, as described above, this would introduce noise that would likely obfuscate the effects that we hypothesized a priori to exist at more proximal social distances. That said, we note that although we constrained our main analyses to dyads four or fewer "degrees of separation" from one another, given our a priori hypotheses, when analyses were repeated without excluding dyads five or more "degrees of separation" from one another, neural similarity was still significantly related to social network proximity across several brain networks. In all cases where connectivity similarity was related to social network proximity, this relationship was positive. This held true when using social distances weighted by emotional closeness, as in our main analyses (*SI Appendix*, Table S12) and when basing social distance on unweighted "degrees of separation" (*SI Appendix*, Table S13).

Subjects indicated whether their alters were their parent, child, grandchild, sibling or "other" relative (e.g., cousin, aunt, etc.). Of the 241 resulting dyads, three dyads consisted of genetically related subjects and were excluded from analyses (two genetically related dyads consisted of siblings and one consisted of "other" relatives). In sum, these 1,778 dyads were excluded from analysis, resulting in 238 unique fMRI dyads, which consisted of 57 fMRI subjects. Ultimately, we analyzed data from these 57 fMRI subjects (35 females, mean age = 70.66, SD = 6.28). The fMRI study was approved by and performed in accordance with the relevant guidelines and regulations by the Institutional Review Board of Yonsei University, and all subjects provided written informed consent for the research procedure.

Image acquisition. Subjects were scanned at the Seoul National University Brain Imaging Center using a 3T Siemens Trio scanner. An echo-planar sequence (2,000-ms repetition time [TR]; 30-ms echo time [TE]; resolution 3.0 × 3.0 × 3.0 mm; gap = 1 mm; field of view 240 × 240 mm) was used to acquire resting-state fMRI data. For each subject, two 5-min runs were acquired, totaling 10 min of data. A high-resolution T1-weighted magnetic prepared rapid gradient echo scan was acquired or each subject (2,300 ms TR; 30 ms TE; field of view 256 × 256 mm; resolution 1 × 1 × 1 mm) at the end of the scanning session.

fMRI data preprocessing. fMRIPrep version 1.1.8 was used for anatomical and functional data preprocessing (70). Each subject's T1-weighted (T1w) image was corrected for intensity nonuniformity with N4BiasFieldCorrection, distributed with ANTs 2.1.0, and used as T1w-reference throughout the workflow. The T1w reference was then skull-stripped with a Nipype implementation of the antsBrainExtraction.sh workflow (from ANTs), using OASIS30ANTs as target template. Spatial normalization to the ICBM 152 Nonlinear Asymmetrical template version 2009c (MNI152NLin2009cAsym) was performed through nonlinear registration with antsRegistration (implemented in ANTs 2.1.0), using brain-extracted versions of both T1w volume and template. Brain tissue segmentation of cerebrospinal fluid (CSF), white matter (WM), and gray matter (GM) was performed on the brain-extracted T1w using FSL FAST.

For each of the two blood oxygen level dependent (BOLD) runs per subject, the following preprocessing was performed. First, a reference volume and its skull-stripped version were generated using a custom methodology of fMRIPrep. The BOLD reference was then coregistered to the T1w reference using FSL FLIRT with the boundary-based registration cost function. Coregistration was configured with nine degrees of freedom to account for distortions remaining in the BOLD reference. Head-motion parameters with respect to the BOLD reference (transformation matrices and six corresponding rotation and translation parameters) were estimated before any spatiotemporal filtering using FSL MCFLIRT. Automatic removal of motion artifacts using independent component analysis (ICA-AROMA) was performed on the preprocessed BOLD in MNI (Montreal Neurological Institute) space time series after removal of nonsteady state volumes and spatial smoothing with an isotropic, Gaussian kernel of 6-mm fullwidth at half maximum. The BOLD time series were then resampled to MNI152NLin2009cAsym standard space, generating a preprocessed BOLD run in MNI152NLin2009cAsym space.

The confounding variables generated by fMRIPrep that were used as nuisance variables in the current study included global signals extracted from within the CSF, WM, and whole-brain masks, framewise displacement, three translational motion parameters, three rotational motion parameters, a basis set of cosine functions up to a cutoff of 128 s, and a set of physiological noise regressors that were extracted to perform component-based noise correction (anatomical CompCor, aCompCor). More specifically, aCompCor variables were calculated within the intersection of a subcortical mask (created by heavily eroding the brain mask) and the union of the CSF and WM masks. These confounds were regressed out of the data for each preprocessed run. Temporal filtering was performed with a band-pass filter between 0.009 and 0.08 Hz.

Functional parcellation and whole-brain connectome construction. To delineate the brain into regions of interest (ROIs), we used the Power et al. (31) atlas with 264 brain regions, 236 of which are associated with one of 13 functionally defined brain networks: visual, auditory, cingulo-opercular task control, cerebellar, dorsal attention, default mode, frontoparietal control, memory retrieval, salience, somatosensory motor-hand, somatosensory motor-mouth, subcortical, and ventral attention networks. Here, only the 236 ROIs associated with the above-mentioned brain networks were used for analysis.

For each subject, in each of the 236 ROIs, the fMRI signal was spatially averaged within a spherical mask (radius = 5 voxels) and extracted at each time point to characterize the neural time series at each brain region. We then calculated the pairwise Pearson correlations between all ROIs' time series in order to construct a symmetric 236 × 236 functional connectivity matrix. This was conducted separately for each of the two resting-state fMRI runs. The two functional connectivity matrices from each run were then Fisher z-transformed and averaged to characterize each subject's whole-brain resting-state functional connectome.

Calculating dyadic similarities in whole-brain connectomes. For each subject, the off-diagonal half of the whole-brain functional connectivity matrix was

flattened into a vector containing 27,730 functional connectivity values. For each of the unique pairs of fMRI subjects, we calculated pairwise Euclidean distances (i.e., absolute value of numerical differences) between the corresponding functional connectivity values in subjects' connectome vectors. We then negated these Euclidean distance values to convert them into similarity values (i.e., higher values reflected higher neural similarity). This resulted in a vector of 27,730 similarity values that characterized whole-brain connectome similarity for each unique pair of fMRI subjects. To account for demographic similarities that may be related to social network proximity and/or similarity in resting-state functional connectivity, prior to all subsequent analyses we regressed out the effects of intersubject similarities in age (i.e., negated Euclidean distance between each pair of individuals' ages) and in gender (i.e., 1: same gender; 0: dissimilar gender) from social network proximity. Significant associations between demographic similarity (as well as personality similarity) and similarity in connectivity within and between functional brain networks are reported in *SI Appendix*, Table S10; significant associations between demographic similarity (as well as personality similarity) and social network proximity are reported in *SI Appendix*, Table S11.

Whole-brain connectome-based predictive modeling of social distance. As described in the main text, we tested if similarities in individuals' distributed patterns of whole-brain resting-state functional connectivity would be predictive of their proximity in their real-world social network, after having controlled for the effects of demographic variables in the previous data analytic step. We used Scikit-learn to implement PLSR (71), a multivariate data-driven regression model that implements dimension reduction by maximizing the covariance between predictors and the response variable to yield latent variables, which are subsequently used as predictors. As such, PLSR is well-suited for datasets whose predictors are characterized by high dimensionality and multicollinearity and is thus a powerful tool to predict response variables using multivariate fMRI data (72, 73).

Scikit-learn's KFold function was used to divide the data into 10 training and test folds (71). Using Scikit-learn's Pipeline function, we created an algorithm that performed three steps in sequence on the training data for each fold (models fit to each fold's training data were used to predict social network proximity based on neural similarities in the corresponding testing data): 1) normalize the predictors using Scikit-learn's RobustScaler function, 2) identify the 1,000 predictors that were mostly strongly associated with social network proximity (as measured using F scores calculated by univariate linear regression between each predictor and social distance), and 3) implement PLSR using these 1,000 predictors. Although PLSR is a robust solution to problems of high dimensionality, performing dimension reduction prior to implementing PLSR improves model performance (74). We used a nested cross-validation scheme to perform hyperparameter tuning using a grid search procedure (i.e., optimizing the n_components hyperparameter from a grid/range of integers ranging from 1 to 10), such that the training data of each of the 10 outer data folds were further subdivided into 10 inner folds consisting of subtraining and validation datasets. Within each of these inner folds, for each hyperparameter value provided in the hyperparameter grid (i.e., n_components values ranging from 1 to 10), the algorithm was trained on the subtraining data and tested on the validation data. The hyperparameter value used in the model with the best performance across all validation sets was identified as the optimal hyperparameter for the corresponding outer training fold. Using this optimal hyperparameter, the algorithm was trained on the outer fold's training data and tested on the outer fold's testing data. This process was repeated for each of the 10 outer data folds. Because each dyad was included in the testing data for one of the outer data folds, this procedure yielded a predicted social network proximity value for each dyad in the sample. Out-of-sample performance was evaluated by calculating the Pearson r value between predicted and actual social distance values. To account for the dependency structure of the data, this r value was then tested against a null distribution of r values generated by permutation testing. Neuroimaging data were randomly shuffled across fMRI participants 5,000 times while holding all else in the dataset constant. In each permuted dataset, the entire data analytic procedure described above (including calculation of dyadic similarities in functional connectomes) was repeated to generate a null distribution of 5,000 r values. P values were determined by calculating the frequency with which the true model's r value exceeded the r values in the null distribution.

To test whether intersubject similarities in functional connectomes would be predictive of social network proximity above and beyond the effects of similarities not only in demographic variables but also in personality traits, we repeated the primary analysis described above while also controlling for interindividual similarities in personality. Personality was assessed using the Big Five 44-item inventory (63), and dyadic similarities in personality were calculated by computing (and negating) the Euclidean distance between individuals' set of five personality traits (i.e., extraversion, agreeableness, consciousness, neuroticism, and openness).

Modeling social network proximity as a function of similarity in functional connectivity at the level of brain networks. To complement our data-driven predictive modeling framework and inform interpretations of these results, we tested the relationships between social network proximity and intersubject similarity in functional connectivity within brain networks and between each possible unique pair of brain networks. To calculate similarity in functional connectivity within each of the 13 functional brain networks defined in the Power et al. (31) atlas, the following procedure was performed for each subject. For each brain network, functional connectivity edges between nodes associated with the brain network were averaged, yielding a single value reflecting the average level of functional connectivity within that brain network. To calculate similarity in functional connectivity between brain networks for each of the 78 possible unique pairs of brain networks, the following procedure was performed for each subject. For each pair of brain networks, functional connectivity values corresponding to edges between nodes associated with each of the two brain networks were averaged, yielding a single value reflecting the average level of functional connectivity between those two brain networks. In total, 91 aggregate functional connectivity values (13 characterizing connectivity within each brain network and 78 characterizing connectivity between each of the unique pairs of brain networks) were calculated for each subject. For each aggregate functional connectivity value, intersubject similarity was computed using Euclidean distance (distance values were negated to convert them to similarity values).

For each brain network and for each unique pair of brain networks (i.e., 91 models total), the relationship between intersubject similarity in functional connectivity and social network proximity was assessed using linear mixed-effects models with crossed random effects (i.e., random intercepts) for both participants to account for dependencies in the data introduced by having repeated observations for each participant. We adopted the method suggested by Chen et al. (32) for analyses of intersubject similarities of fMRI data, which was implemented using lme4 and lmerTest in R (75, 76). The intersubject similarity data were doubled to allow for crossed random effects, as suggested by Chen et al. (32). For statistical inference, to avoid inflating degrees of freedom due to the resultant data redundancy, degrees of freedom were then corrected as suggested and validated by Chen et al. (32)—for example, the degrees of freedom for the SE were adjusted from $(2N - k - 1)$ to $(N - k - 1)$, where k is the number of fixed effects in the model and N is the number of observations (dyads). SEs were adjusted with a scaling factor of $\sqrt{2N-1}/\sqrt{N-1}$, where N is the number of participants. All reported findings reflect results using the corrected degrees of freedom and SE estimates. FDR correction was then implemented to correct for multiple comparisons across all 91 statistical tests.

Exploratory moderation analysis. Exploratory analyses tested whether geographic distance moderated the relationship between connectome similarity and social network proximity. For a given pair of subjects, geographic distance was calculated by computing the walking distance in meters between the geographic coordinates encoding the location of residence for each individual. The significance of the main effect of geographic distance on social network proximity, as well as the interaction between geographic distance and neural similarity on social network proximity, was assessed using linear mixed-effects models (using the approach described in the preceding section) that contained fixed effects for neural similarity (described in more detail below), geographic distance, and their interaction and crossed random effects for both participants in each dyad. We carried out this procedure using two approaches to characterize neural similarity: 1) using the primary PLS component (to approximate the neural similarity data used in the predictive modeling analyses) and 2) using the aggregate neural similarity measures from the nine models in which similarity in functional connectivity within and between brain networks was associated with social network proximity (Table 1).

In the first approach, we implemented a PLSR-based algorithm to characterize the connectome similarity variable. We first identified the modal *n_components* value across all 10 data folds in the main analysis. In a separate implementation of the PLSR-based algorithm, we then set the *n_components* value equal to the aforementioned modal value. This algorithm then used connectome similarity across the entire sample to predict social network proximity across the entire sample, and the primary PLS component was extracted to be used as the neural similarity variable in the moderation analysis. A cross-validation scheme was not used here, as it would have produced multiple sets of different PLS components. Therefore, this analysis is not used to assess the significance of the relationship between neural similarity and social network proximity and is used only to assess how

this relationship differs as a function of geographic distance for the aspects of neural connectivity that are associated with social network proximity.

This process yielded latent variables that maximized the covariance between all of the functional connectivity-based predictors and social network proximity. We extracted the latent variable that best maximized this covariance, and we then used this single variable as the connectome similarity variable in approach 1 of the moderation analysis. This procedure was used to obtain a single variable that approximated the overall characterization of functional connectome similarity obtained in the predictive modeling analysis (as this variable necessarily varied across data folds in the predictive modeling analysis), so that the impact of geographic distance on the relationship between this aggregate variable and social network proximity could be explored. Given this procedure for deriving this aggregate connectome similarity measure, inferences regarding the relationship between neural similarity and social network proximity should be based on the analyses described in the preceding sections (rather than the main effect of neural similarity in this analysis or the extent to which each simple slope differs from 0). This exploratory analysis is specifically focused on examining how, for neural variables that are related to social network proximity, the relationship between functional connectivity similarity and social network proximity varies as a function of geographic distance.

We followed the common convention (77, 78) of visualizing slopes at three levels of the moderator (the mean ± 1 SD). However, given that the smallest geographic proximity values in this dataset were 0.958 SD below the mean, this is the precise value of geographic proximity used for characterizing and visualizing the simple slope for participants who lived particularly close to one another (rounded down to −1 SD below mean in the legend of Fig. 4 for simplicity).

Data Availability. Anonymized fMRI, social network, and questionnaire data and code used for analyses have been deposited in a GitHub repository (https://github.com/rhhyon/KSHAP-PNAS-2020).

ACKNOWLEDGMENTS. We thank Dr. Elisa Baek and João Guassi Moreira for helpful discussion. This work was supported by the National Research Foundation of Korea (NRF-2017S1A3A2067165) and Yonsei University Research Grant of 2020 (Y.Y.) and a Sloan Foundation Research Fellowship (C.P.).

1. M. McPherson, L. Smith-Lovin, J. M. Cook, Birds of a feather: Homophily in social networks. *Annu. Rev. Sociol.* **27**, 415–444 (2001).
2. D. C. Feiler, A. M. Kleinbaum, Popularity, similarity, and the network extraversion bias. *Psychol. Sci.* **26**, 593–603 (2015).
3. M. Selfhout, J. Denissen, S. Branje, W. Meeus, In the eye of the beholder: Perceived, actual, and peer-rated similarity in personality, communication, and friendship intensity during the acquaintanceship process. *J. Pers. Soc. Psychol.* **96**, 1152–1165 (2009).
4. O. Miranda-Dominguez *et al*., Connectotyping: Model based fingerprinting of the functional connectome. *PLoS One* **9**, e111048 (2014).
5. E. S. Finn *et al*., Functional connectome fingerprinting: Identifying individuals using patterns of brain connectivity. *Nat. Neurosci.* **18**, 1664–1671 (2015).
6. D. E. Meskaldji *et al*., Prediction of long-term memory scores in MCI based on resting-state fMRI. *Neuroimage Clin.* **12**, 785–795 (2016).
7. R. E. Beaty *et al*., Robust prediction of individual creative ability from brain functional connectivity. *Proc. Natl. Acad. Sci. U.S.A.* **115**, 1087–1092 (2018).
8. M. D. Rosenberg *et al*., A neuromarker of sustained attention from whole-brain functional connectivity. *Nat. Neurosci.* **19**, 165–171 (2016).
9. M. D. Rosenberg, W. T. Hsu, D. Scheinost, R. Todd Constable, M. M. Chun, Connectome-based models predict separable components of attention in novel individuals. *J. Cogn. Neurosci.* **30**, 160–173 (2018).
10. L. Christov-Moore, N. Reggente, P. K. Douglas, J. D. Feusner, M. Iacoboni, Predicting empathy from resting state brain connectivity: A multivariate approach. *Front. Integr. Nuerosci.* **14**, 3 (2020).
11. J. Dubois, P. Galdi, Y. Han, L. K. Paul, R. Adolphs, Resting-state functional brain connectivity best predicts the personality dimension of openness to experience. *Personal. Neurosci.* **1**, e6 (2018).
12. J. M. Lahnakoski *et al*., Synchronous brain activity across individuals underlies shared psychological perspectives. *Neuroimage* **100**, 316–324 (2014).
13. J. F. Cantlon, R. Li, Neural activity during natural viewing of Sesame Street statistically predicts test scores in early childhood. *PLoS Biol.* **11**, e1001462 (2013).
14. Y. Yeshurun *et al*., Same story, different story: The neural representation of interpretive frameworks. *Psychol. Sci.* **28**, 307–319 (2017).
15. C. Parkinson, A. M. Kleinbaum, T. Wheatley, Similar neural responses predict friendship. *Nat. Commun.* **9**, 332 (2018).
16. R. Hyon, A. M. Kleinbaum, C. Parkinson, Social network proximity predicts similar trajectories of psychological states: Evidence from multi-voxel spatiotemporal dynamics. *Neuroimage* **216**, 116492 (2020).
17. E. B. Falk, D. S. Bassett, Brain and social networks: Fundamental building blocks of human experience. *Trends Cogn. Sci.* **21**, 674–690 (2017).
18. M. Moussaïd, H. Brighton, W. Gaissmaier, The amplification of risk in experimental diffusion chains. *Proc. Natl. Acad. Sci. U.S.A.* **112**, 5631–5636 (2015).
19. M. Moussaïd, S. M. Herzog, J. E. Kämmer, R. Hertwig, Reach and speed of judgment propagation in the laboratory. *Proc. Natl. Acad. Sci. U.S.A.* **114**, 4117–4122 (2017).
20. N. A. Christakis, J. H. Fowler, The spread of obesity in a large social network over 32 years. *N. Engl. J. Med.* **357**, 370–379 (2007).
21. J. H. Fowler, N. A. Christakis, Cooperative behavior cascades in human social networks. *Proc. Natl. Acad. Sci. U.S.A.* **107**, 5334–5338 (2010).
22. N. A. Christakis, J. H. Fowler, The collective dynamics of smoking in a large social network. *N. Engl. J. Med.* **358**, 2249–2258 (2008).
23. J. N. Rosenquist, J. H. Fowler, N. A. Christakis, Social network determinants of depression. *Mol. Psychiatry* **16**, 273–281 (2011).
24. J. T. Cacioppo, J. H. Fowler, N. A. Christakis, Alone in the crowd: The structure and spread of loneliness in a large social network. *J. Pers. Soc. Psychol.* **97**, 977–991 (2009).
25. M. W. Cole, T. Yarkoni, G. Repovš, A. Anticevic, T. S. Braver, Global connectivity of prefrontal cortex predicts cognitive control and intelligence. *J. Neurosci.* **32**, 8988–8999 (2012).
26. J. H. Fowler, N. A. Christakis, Dynamic spread of happiness in a large social network: Longitudinal analysis over 20 years in the Framingham Heart Study. *BMJ* **338**, 23–26 (2009).
27. O. P. John, L. P. Naumann, C. J. Soto, "Paradigm shift to the integrative big-five trait taxonomy: History, measurement, and conceptual issues" in *Handbook of Personality: Theory and Research*, O. P. John, R. W. Robins, L. A. Pervin, Eds. (Guilford Press, 2008), pp. 114–158.
28. S. V Paunonen, Big Five factors of personality and replicated predictions of behavior. *J. Pers. Soc. Psychol.* **84**, 411–424 (2003).
29. Y. Youm *et al*., Social network properties and self-rated health in later life: Comparisons from the Korean social life, health, and aging project and the national social life, health and aging project. *BMC Geriatr.* **14**, 102 (2014).
30. J.-M. Lee *et al*., The Korean social life, health and aging project-health examination cohort. *Epidemiol. Health* **36**, e2014003 (2014).
31. J. D. Power *et al*., Functional network organization of the human brain. *Neuron* **72**, 665–678 (2011).
32. G. Chen, P. A. Taylor, Y. W. Shin, R. C. Reynolds, R. W. Cox, Untangling the relatedness among correlations, Part II: Inter-subject correlation group analysis through linear mixed-effects modeling. *Neuroimage* **147**, 825–840 (2017).
33. L. Nahemow, M. P. Lawton, Similarity and propinquity in friendship formation. *J. Pers. Soc. Psychol.* **32**, 205–213 (1975).
34. J. Mossong *et al*., Social contacts and mixing patterns relevant to the spread of infectious diseases. *PLoS Med.* **5**, e74 (2008).
35. A. Stopczynski, A. 'S.' Pentland, S. Lehmann, How physical proximity shapes complex social networks. *Sci. Rep.* **8**, 1–10 (2018).
36. C. Horien, X. Shen, D. Scheinost, R. T. Constable, The individual functional connectome is unique and stable over months to years. *Neuroimage* **189**, 676–687 (2019).
37. W. Liu, N. Kohn, G. Fernández, Intersubject similarity of personality is associated with intersubject similarity of brain connectivity patterns. *Neuroimage* **186**, 56–69 (2019).
38. C. J. Vaidya, E. M. Gordon, Phenotypic variability in resting-state functional connectivity: Current status. *Brain Connect.* **3**, 99–120 (2013).
39. A. Otti *et al*., I know the pain you feel-how the human brain's default mode predicts our resonance to another's suffering. *Neuroscience* **169**, 143–148 (2010).
40. M. Rossignac-Milon, N. Bolger, K. S. Zee, E. J. Boothby, E. T. Higgins, Merged minds: Generalized shared reality in dyadic relationships. *J. Pers. Soc. Psychol.* (2020).
41. G. Pagnoni, Dynamical properties of BOLD activity from the ventral posteromedial cortex associated with meditation and attentional skills. *J. Neurosci.* **32**, 5242–5249 (2012).
42. C. L. Apicella, F. W. Marlowe, J. H. Fowler, N. A. Christakis, Social networks and cooperation in hunter-gatherers. *Nature* **481**, 497–501 (2012).
43. J.-P. Onnela, S. Arbesman, M. C. González, A.-L. Barabási, N. A. Christakis, Geographic constraints on social network groups. *PLoS One* **6**, e16939 (2011).
44. D. Liben-Nowell, J. Novak, R. Kumar, P. Raghavan, A. Tomkins, Geographic routing in social networks. *Proc. Natl. Acad. Sci. U.S.A.* **102**, 11623–11628 (2005).
45. R. Lambiotte *et al*., Geographical dispersal of mobile communication networks. *Phys. A Stat. Mech. Appl.* **387**, 5317–5325 (2008).
46. C. R. Berger, R. J. Calabrese, Some explorations in initial interaction and beyond: Toward a developmental theory of interpersonal communication. *Hum. Commun. Res.* **1**, 99–112 (1975).
47. G. L. Clore, D. A. Byrne, "A reinforcement-affect model of attraction" in *Foundations of Interpersonal Attraction*, T. L. Huston, Ed. (Academic Press, 1974), pp. 143–165.
48. E. Redcay, L. Schilbach, Using second-person neuroscience to elucidate the mechanisms of social interaction. *Nat. Rev. Neurosci.* **20**, 495–505 (2019).
49. D. Bolis, J. Balsters, N. Wenderoth, C. Becchio, L. Schilbach, Beyond autism: Introducing the dialectical misattunement hypothesis and a Bayesian account of intersubjectivity. *Psychopathology* **50**, 355–372 (2017).
50. J. M. Lahnakoski, P. A. G. Forbes, C. McCall, L. Schilbach, Unobtrusive tracking of interpersonal orienting and distance predicts the subjective quality of social interactions. *R. Soc. Open Sci.* **7**, 191815 (2020).
51. R. B. Cialdini, N. J. Goldstein, Social influence: Compliance and conformity. *Annu. Rev. Psychol.* **55**, 591–621 (2004).
52. F. B. M. de Waal, "The 'Russian Doll' model of empathy and imitation" in *On Being Moved: From Mirror Neurons to Empathy*, S. Braten, Ed. (John Benjamins, 2007), pp. 49–69.

53. C. Cattuto *et al*., Dynamics of person-to-person interactions from distributed RFID sensor networks. *PLoS One* **5**, e11596 (2010).
54. A. P. Mackey, A. T. Miller Singley, S. A. Bunge, Intensive reasoning training alters patterns of brain connectivity at rest. *J. Neurosci.* **33**, 4796–4803 (2013).
55. C. B. McNabb *et al*., No evidence for a relationship between social closeness and similarity in resting-state functional brain connectivity in schoolchildren. *Sci. Rep.* **10**, 10710 (2020).
56. E. S. Finn *et al*., Can brain state be manipulated to emphasize individual differences in functional connectivity? *Neuroimage* **160**, 140–151 (2017).
57. M. B. O'Donnell, J. B. Bayer, C. N. Cascio, E. B. Falk, Neural bases of recommendations differ according to social network structure. *Soc. Cogn. Affect. Neurosci.* **12**, 61–69 (2017).
58. R. Schmälzle *et al*., Brain connectivity dynamics during social interaction reflect social network structure. *Proc. Natl. Acad. Sci. U.S.A.* **114**, 5153–5158 (2017).
59. G. J. Stephens, L. J. Silbert, U. Hasson, Speaker-listener neural coupling underlies successful communication. *Proc. Natl. Acad. Sci. U.S.A.* **107**, 14425–14430 (2010).
60. L. Schilbach, Towards a second-person neuropsychiatry. *Philos. Trans. R. Soc. B Biol. Sci.* **371**, 20150081 (2016).
61. M. F. Green *et al*., Social disconnection in schizophrenia and the general community. *Schizophr. Bull.* **44**, 242–249 (2018).
62. W. T. Joo, S. Kwak, Y. Youm, J. Chey, Brain functional connectivity difference in the complete network of an entire village: The role of social network size and embeddedness. *Sci. Rep.* **7**, 4465 (2017).
63. S. Y. Kim *et al*., Standardization and validation of Big five inventory-Korean version (BFI-K) in elders. *Korean J. Biol. Psychiatry* **17**, 15–25 (2016).
64. G. Csárdi, T. Nepusz, The igraph software package for complex network research. *InterJournal Complex Syst.* **Complex Systems**, 1695 (2014).
65. E. W. Dijkstra, A note on two problems in connexion with graphs. *Numer. Math.* **1**, 269–271 (1959).
66. J. Han *et al*., A normative study of the mini-mental state examination for dementia screening (MMSE-DS) and its short form (SMMSE-DS) in the Korean elderly. *J. Korean Geriatr. Psychiatry* **14**, 27–37 (2010).
67. J. Chey, *Elderly Memory Disorder Scale* (Hakjisa, Seoul, 2007).
68. J. C. Morris, The clinical dementia rating (CDR): Current version and scoring rules. *Neurology* **43**, 2412–2414 (1993).
69. N. A. Christakis, J. H. Fowler, Social contagion theory: Examining dynamic social networks and human behavior. *Stat. Med.* **32**, 556–577 (2013).
70. O. Esteban *et al*., fMRIPrep: A robust preprocessing pipeline for functional MRI. *Nat. Methods* **16**, 111–116 (2019).
71. F. Pedregosa *et al*., Scikit-learn: Machine learning in Python. *J. Mach. Learn. Res.* **12**, 2825–2830 (2011).
72. A. Krishnan, L. J. Williams, A. R. McIntosh, H. Abdi, Partial least squares (PLS) methods for neuroimaging: A tutorial and review. *Neuroimage* **56**, 455–475 (2011).
73. A. R. McIntosh, B. Mišić, Multivariate statistical analyses for neuroimaging data. *Annu. Rev. Psychol.* **64**, 499–525 (2013).
74. T. Mehmood, K. H. Liland, L. Snipen, S. Sæbø, A review of variable selection methods in Partial Least Squares Regression. *Chemom. Intell. Lab. Syst.* **118**, 62–69 (2012).
75. A. Kuznetsova, P. B. Brockhoff, R. H. B. Christensen, lmerTest package: Tests in linear mixed effects models. *J. Stat. Softw.* **82**, 1–26 (2017).
76. D. Bates, M. Mächler, B. M. Bolker, S. C. Walker, Fitting linear mixed-effects models using lme4. *J. Stat. Softw.* **67**, 1–48 (2015).
77. L. S. Aiken, S. G. West, *Multiple Regression: Testing and Interpreting Interactions* (SAGE Publications Inc., 1991).
78. J. Cohen, P. Cohen, S. G. West, L. S. Aiken, *Applied Multiple Regression/Correlation Analysis for the Behavioral Sciences* (Lawrence Erlbaum Associates, ed. 3, 2003).